Kinetics and Catalysis, Vol. 41, No. 3, 2000, pp. 340–348. Translated from Kinetika i Kataliz, Vol. 41, No. 3, 2000, pp. 375–384.

Kinetics and Mechanism of Water Catalytic Oxidation by a $Ru^{3+}(bpy)_3$ Complex in the Presence of Colloidal Cobalt Hydroxide

O. P. Pestunova, G. L. Elizarova, and V. N. Parmon

Boreskov Institute of Catalysis, Siberian Division, Russian Academy of Sciences, Novosibirsk, 630090 Russia

Received November 13, 1998

Abstract—Kinetics of the catalytic oxidation of water to molecular oxygen by a tris(bipyridyl) Ru(III) complex is studied in the presence of colloidal cobalt hydroxide stabilized by starch. Oxidant consumption follows the first-order rate law with respect to the oxidant concentration. The dependence of the apparent rate constant of this process on the catalyst concentration, initial oxidant concentration, and initial concentration of its reduced form was determined. The dependence of the oxygen yield on H^+ at pH 7–11 and a catalyst concentration of 10^{-7}–10^{-3} mol/l is studied. An intermediate product of the reaction was found, which is probably a bridged peroxo complex of cobalt. The kinetic scheme and mechanism of the reaction is proposed, which agree with experimental observations.

INTRODUCTION

The catalytic oxidation of water to oxygen by one-electron oxidants, such as a tris(bipyridyl) Ru(III) complex,

$$4Ru^{3+}(bpy)_3 + 2H_2O \longrightarrow 4Ru^{3+}(bpy)_3 + O_2 + 4H^+, \quad (I)$$

was studied over 20 years in connection with artificial photocatalytic systems for water decomposition and simulation of the oxygen-producing complex of photosystem II of green plants. There are some achievements in designing and studying catalysts for this reaction. However, there is no agreement on the mechanism of reaction (I).

Most of the work done along this line is devoted to the kinetic and mechanistic studies of reaction (I) in neutral and weakly alkaline media with $CoCl_2$ as a catalyst [1–3]. The interpretation of the results of these studies was difficult because the true catalysts of this reaction are Co(III) hydroxo complexes, which are formed during the reaction by the interaction of aqua ions of Co(II) with an oxidant and hydroxyls.

Earlier, we studied the mechanism of water oxidation in the presence of supported Co(III), Mn(III), Fe(III), and Ru(IV)-containing hydroxide catalysts [4, 5]. We hypothesized that the action of catalysts based on transition metal hydroxyls is similar for all metal ions. Quantum chemical calculations suggested that the intermediates formed in the reaction of water oxidation are peroxide complexes [6, 7].

This paper reports kinetic data on reaction (I) and oxygen yield in the presence of a colloidal Co(III) hydroxide catalyst stabilized by modified starch [8]. The application of this catalyst makes it possible to avoid problems associated with the stage of catalyst formation during the process and to extend the ranges of pH and concentrations at which the catalyst works. We also obtained new data on the intermediate catalyst states in the reaction.

EXPERIMENTAL

The following analytical purity grade reagents were used without additional purification: $HClO_4$, Na_2HPO_4, KH_2PO_4, $NaClO_4$, $KHCO_3$, and bipyridyl, as well as extra purity grade H_3BO_3 and NaOH. Analytical purity grade starch for iodometry was modified by heating for 8 h at 430 K [8]. Phospate and borate buffer solutions were prepared as described in [9]. The $Ru(bpy)_3(ClO_4)_2 \cdot 2H_2O$ complex was prepared according to the published technique [10]. $Ru(bpy)_3(ClO_4)_3$ was prepared by the oxidation of the Ru(II) complex by tin dioxide [11]. The $KCo(NH_3)_2(CO_3)_2$ complex, which is necessary for the preparation of the colloidal catalyst, was obtained according to the procedure described in [12].

The colloidal cobalt hydroxide stabilized by modified starch was prepared according to our technique described in [8].

In kinetic experiments on hydrogen evolution at high pH in the presence of small catalyst amounts, we used doubly distilled water for the preparation of solutions. In all other catalytic and kinetic experiments and in catalyst preparation, we used distilled water.

The concentration of O_2 in solutions was measured by the Clark electrode using a Beckman Monitor II instrument according to the technique described in [8]. For pH measurements, an EV-74 pH-meter was used.

0023-1584/00/4103-0340$25.00 © 2000 MAIK "Nauka/Interperiodica"

Kinetic experiments were carried out in a constant-temperature cell (298 K) 0.2 cm long, using a stopped-flow SF-3L setup with a temporal resolution of 10 ms. The kinetics of water oxidation by $Ru(bpy)_3(ClO_4)_3$ was studied by spectrophotometry by monitoring a decrease in the intensity of the oxidant band at $\lambda = 675$ nm or by an increase in the intensity of the reduced form band at $\lambda = 452$ nm ($\varepsilon = 400$ and 14 000, respectively).

For the stopped-flow experiments, two solutions were prepared: (1) the oxidant $Ru(bpy)_3(ClO_4)_3$ solution or its mixture with the reduced form $Ru(bpy)_3(ClO_4)_2 \cdot 2H_2O$ with water (if necessary) and (2) the catalyst solution in a 0.06 mol/l borate buffer (pH 9.2). These solutions were mixed by injection into the cell. The signal from a photomultiplier tube was registered with a S9-8 oscilloscope. The absorbances of solutions were calculated by comparison of the measured signal with that measured at the final state. The latter was measured by an ordinary spectrophotometer. The formula for absorbance calculation is

$$D_x = D_f - \ln(U_x/U_f),$$

where D_x and D_f are unknown and final absorbances and U_x and U_f are the amplitudes of the potential signal registered by the photomultiplier tube for the current and final states of the solution.

RESULTS AND DISCUSSION

Dependence of the Oxygen Yield on Experimental Conditions

The dependence of the oxygen yield on the catalyst concentration provides information on the ratio of the rates of oxygen molecule formation and side reactions of catalytic and stoichiometric oxidant destruction because of organic ligand (bipyridyl, bpy) oxidation. If the catalytic destruction does not occur with an increase in the catalyst concentration, the yield of oxygen should grow monotonically up to 100% with respect to the yield expected from the stoichiometry of reaction (I). However, as previous studies showed, this is never observed [1, 3, 8, 13]. The dependence of the oxygen yield in reaction (I) on the catalyst concentration usually has a volcano shape. Even under the most favorable conditions, the maximal yield of oxygen never reached 100%. This fact points to the presence of common steps and intermediates in water oxidation and bipyridyl destruction.

We measured the yields of oxygen over wide ranges of catalyst concentration (10^{-7}–10^{-3} mol/l) at two different initial concentrations of the oxidant (5×10^{-4} and 10^{-3} mol/l) at pH 7, 9, and 11. Figure 1 shows that the yield of O_2 grows at all pH with an increase in the catalyst concentration and reaches the maxima at a molar oxidant/catalyst ratio of 10–100. Then, the yield decreases with a further increase in the catalyst concentration, probably because of Co(III) hydroxide-catalyzed side reactions. At pH 7, the maximal yield of O_2 is ~55–60% and decreases to zero at the equimolar oxidant/catalyst ratio. At pH 9 and 11 and a molar oxidant/catalyst ratio of 10–100, the maximal yield of O_2 reaches 75 and 85%, respectively. When the catalyst concentration is increased to values close to the oxidant concentration, the yield decreases only slightly. Note that, at pH 11, the yield of oxygen varies between 65 and 85%, while the concentration of cobalt hydroxide changes by two orders of magnitude (from 5×10^{-5} to 10^{-3} mol/l). However, in this case, the yield does not reach 100%. The maxima of the O_2 yield were also observed at certain catalyst concentrations in [14].

Stopped-Flow Kinetic Study

Kinetics of $Ru^{3+}(bpy)_3$ consumption under the conditions of its excess over the catalyst. Kinetics was studied at pH 9.2 at oxidant concentrations of 10^{-5}–10^{-3} mol/l and catalyst concentrations of 10^{-7}–10^{-3} mol/l. Unfortunately, at pH 11, studies were impossible because the reaction rate was so high under these conditions that the stopped-flow method failed to measure the rates: the characteristic times of transformations are tens of milliseconds or shorter.

At low concentrations of the catalyst (below 5×10^{-5} mol/l), the kinetic curves of oxidant consumption measured by the absorbance at 675 nm and reduced form formation (452 nm) had exponential forms and corresponded to the first-order reaction with respect to the oxidant. Figure 2 shows linearized plots on a semilogarithmic scale for oxidant consumption and $Ru^{2+}(bpy)_3$ formation. The corresponding apparent rate constants k_{app} calculated from these curves are as follows:

$[Co]_\Sigma \times 10^5$, mol/l	k_{app}, s^{-1}	
	$\lambda = 675$ nm	$\lambda = 450$ nm
3.8	60.5	84.9
1.3	27.6	27.2
0.5	10.9	10.7

Within the limits of the experimental error, the apparent rate constants calculated from oxidant consumption and $Ru(bpy)_3$ formation data are the same.

The exponential form of kinetic curves for oxidant consumption and reduced form formation is rather unexpected, because all previous reports on reaction (I) contained information on retardation of the reaction by the reduced form of the oxidant (i.e., by the $Ru^{2+}(bpy)_3$ complex).

The dependence of the apparent rate constant on the concentration of the colloidal catalyst is linear over the whole range of Co(III) concentrations (5×10^{-6}–5×10^{-5} mol/l), which is typical of catalytic processes. Figure 3 shows the dependence of k_{app} on the initial concentration of the oxidant at 10^{-5}–10^{-3} mol/l $Ru^{3+}(bpy)_3$ for two different catalyst concentrations. The apparent rate constants decrease with an increase in the oxidant

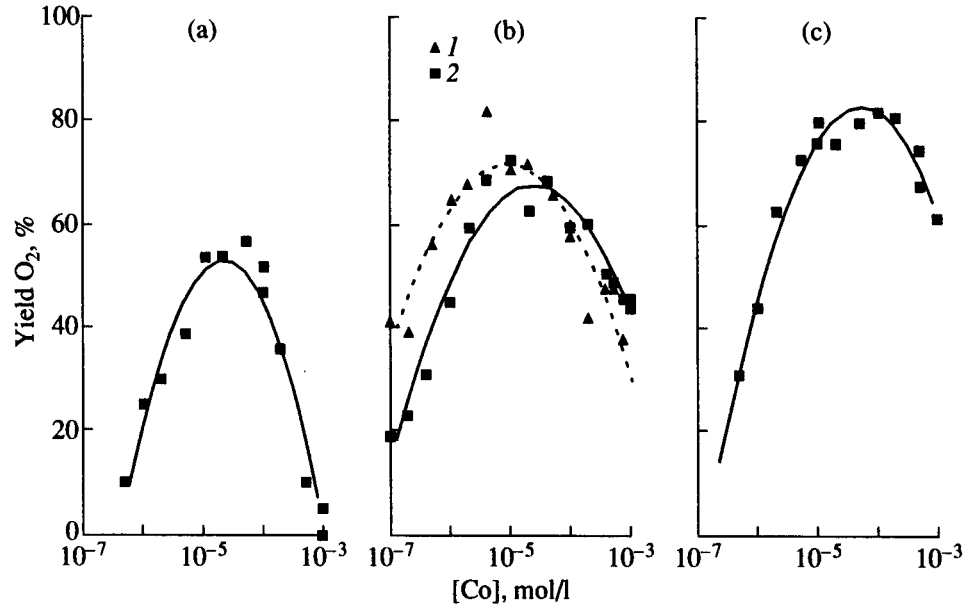

Fig. 1. Oxygen yield vs. catalyst concentration at different pH and initial oxidant concentrations: (a) 0.05 mol/l phosphate buffer, pH 7, $[Ru^{3+}(bpy)_3]_0 = 1 \times 10^{-3}$ mol/l; (b) 0.05 mol/l borate buffer, pH 9.2, (*1*) $[Ru^{3+}(bpy)_3]_0 = 5 \times 10^{-4}$ mol/l and (2) $[Ru^{3+}(bpy)_3]_0 = 1 \times 10^{-3}$ mol/l; (c) pH 11, no buffer, $[Ru^{3+}(bpy)_3]_0 = 1 \times 10^{-3}$ mol/l.

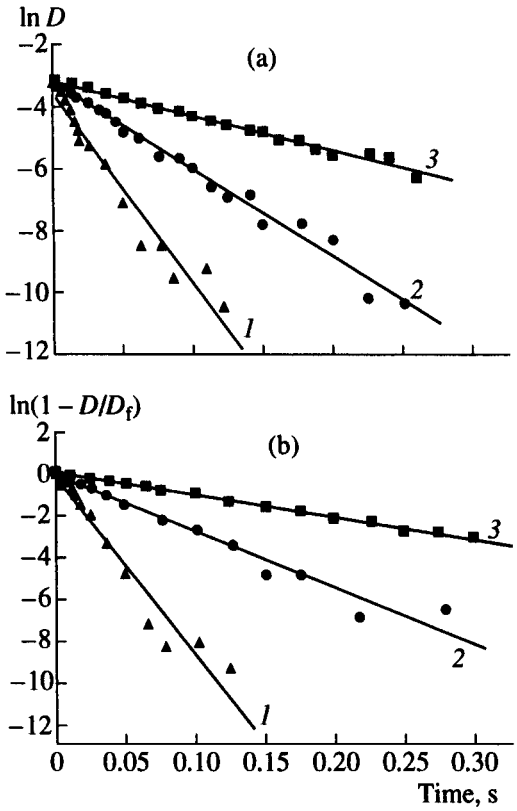

Fig. 2. Typical absorbances D of the catalytic system on a semilogarthimic scale at (a) $\lambda = 675$ and (b) 450 nm and catalyst concentrations $[Co]_\Sigma$ of (*1*) 3.8×10^{-5}, (*2*) 1.3×10^{-5}, and (*3*) 5.0×10^{-6} mol/l ($[Ru^{3+}(bpy)_3]_0 = 5 \times 10^{-4}$ mol/l, 0.03 mol/l borate buffer, pH 9.2). D_f is the final absorbance.

concentration, and $1/k_{app}$ depends on the initial concentration of $Ru^{3+}(bpy)_3$.

The addition of $Ru^{2+}(bpy)_3$ to the initial solution results in the slight retardation of the reaction and does not change the exponential character of the kinetic curves of oxidant consumption. Figure 4 shows the dependence of k_{app} on the initial concentration of $Ru^{2+}(bpy)_3$. This constant decreases with an increase in the concentration of the complex, and $1/k_{app}$ linearly depends on $[Ru^{2+}(bpy)_3]$. As noted above, apparent retardation is rather weak. This becomes virtually unnoticeable if the initial concentration of $Ru^{3+}(bpy)_3$ is more than 10 times higher than the initial concentration of $Ru^{2+}(bpy)_3$.

Reaction kinetics at high conentrations of the catalyst. At high concentrations of the catalyst, kinetic curves of oxidant consumption constructed from changes of the respective band intensity at $\lambda = 675$ nm differ from those obtained at low catalyst concentrations. At a catalyst concentration of 5×10^{-5}–2.5×10^{-4} mol/l, two regions are clearly seen on kinetic curves (Fig. 5). The first region is the fast disappearance of the oxidant, and the second region corresponds to its slow disappearance after 80–90% oxidant consumption. Simultaneously, an increase in the intensity at $\lambda = 452$ nm is observed, which points to the appearance of the $Ru^{2+}(bpy)_3$ complex. This process is described by the first-order rate law with a rate constant equal to that corresponding to the "fast region" on the kinetic curve for $\lambda = 675$ nm.

We may assume that the "slow" region of the kinetic curve registered at $\lambda = 675$ nm is the disappearance of

the intermediate in water oxidation rather than the oxidant. These two species absorb in the same spectral region. Moreover, at [Co] > 2.5×10^{-4} mol/l, when it is impossible to register the formation of the reduced oxidant form because of short characteristic times as compared to the temporal resolution of our setup, only the disappearance of this intermediate is observed at 675 nm with a first-order rate constant of ~2 s^{-1}.

We reconstructed the spectrum of intermediate species consumption using experimental points. To do that, we registered kinetic curves of absorbance changes at wavelengths from 460 to 680 nm at 20-nm intervals. To construct the spectrum, we used the absorbance at the instant $Ru^{3+}(bpy)_3$ was completely consumed. Figure 6 shows the spectrum of intermediate species consumption obtained at catalyst and oxidant concentrations of 4×10^{-4} and 5×10^{-4} mol/l, respectively. Because 99% of the oxidant is consumed for ~58 ms (k_{app} ~ 80 s^{-1}) under these conditions, we measured the absorbance every 100 ms starting from the instant the reactants were mixed to obtain the spectrum for the intermediate species. The optical spectrum of the intermediate is a broad band with an indistinct maximum at 550–600 nm (Fig. 6). Khannanov *et al.* [15] also discovered an intermediate of reaction (I) in the presence of cobalt salts, but its absorbance was near 800 nm. They concluded that this intermediate is the product of oxidant destruction.

The absorbance of the intermediate found in this work is proportional to the concentrations of the catalyst and oxidant. Thus, as the catalyst concentration increases from 1.3×10^{-4} to 1×10^{-3} mol/l at a constant initial concentration of $Ru^{3+}(bpy)_3$ of 10^{-3} mol/l, the absorbance at $\lambda = 675$ nm increases by a factor of ~2.5. As this takes place, the rate of intermediate species consumption remains virtually the same, and the rate constant of this process is ~2.0 s^{-1}. At a constant catalyst concentration of 10^{-4} mol/l and with an increase in the concentration of $Ru^{3+}(bpy)_3$ from 2×10^{-4} to 2×10^{-3} mol/l, the intermediate species absorbance at the same wavelength increases by a factor of ~5. Figure 7 shows the intermediate species absorbance at $\lambda = 568$ nm (in the isobestic point of absorption spectra for $Ru^{3+}(bpy)_3$ and $Ru^{2+}(bpy)_3$). Note that it was rather difficult to identify the appearance of this intermediate because, at high concentrations of the catalyst and intermediate, the rate of intermediate species formation was outside the limits of the temporal resolution of our stopped-flow setup.

Because the absorbance is proportional to the concentrations of the catalyst and oxidant, it is reasonable to suppose that the intermediate is the product of catalyst and oxidant interaction. This is either the product of the partial oxidation of water, which is coordinated to the active center of the catalyst or the product of a side reaction of catalytic oxidant destruction, that is, a ruthenium complex with partially oxidized ligands. It is important that the absorption spectrum of this intermediate is rather broad, which is more characteristic of

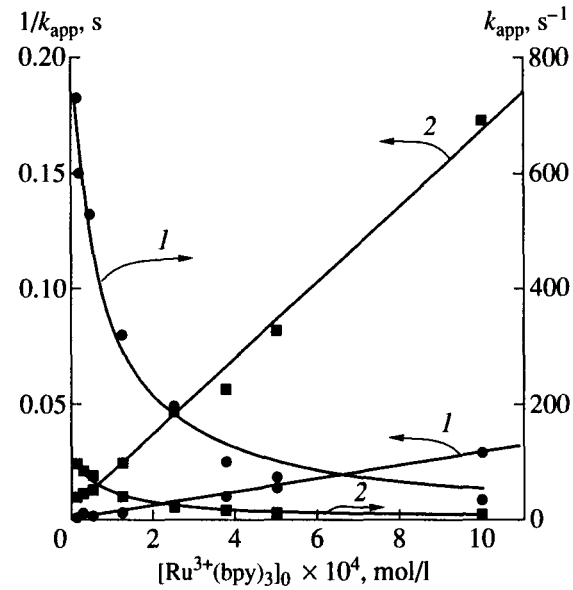

Fig. 3. A plot of k_{app} and $1/k_{app}$ vs. $Ru^{3+}(bpy)_3$ initial concentration at (*1*) $[Co]_\Sigma$ 2.5×10^{-4} mol/l and (*2*) 5×10^{-6} mol/l in 0.03 mol/l borate buffer at pH 9.2.

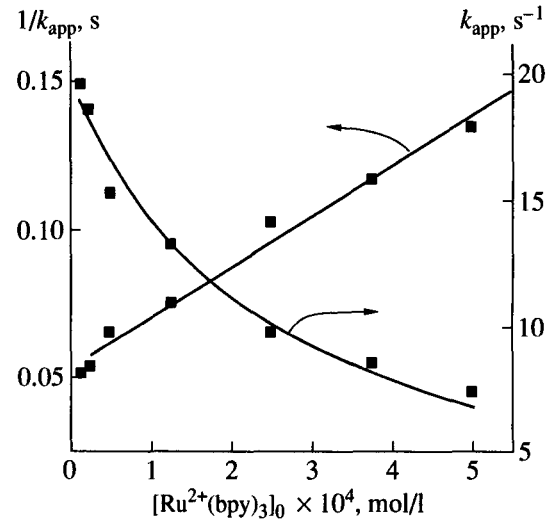

Fig. 4. A plot of k_{app} and $1/k_{app}$ vs. $Ru^{2+}(bpy)_3$ initial concentration at $[Co]_\Sigma = 5 \times 10^{-6}$ mol/l and $[Ru^{3+}(bpy)_3]_0 = 2.5 \times 10^{-4}$ mol/l in 0.03 mol/l borate buffer at pH 9.2.

colloids rather than individual metal complexes. Moreover, most Ru(II) complexes with bipyridyl or similar ligands absorb in the region of shorter wavelengths and have extinction coefficients above 10 000, whereas the estimate of the extinction coefficient gives a value of several hundreds. Taking this into account, we may assume that the intermediate registered in our work is a peroxo complex of colloidal cobalt hydroxide.

Mechanism of Water Oxidation

Kinetic scheme of reaction for the case of low catalyst concentration. The following scheme (Scheme 1)

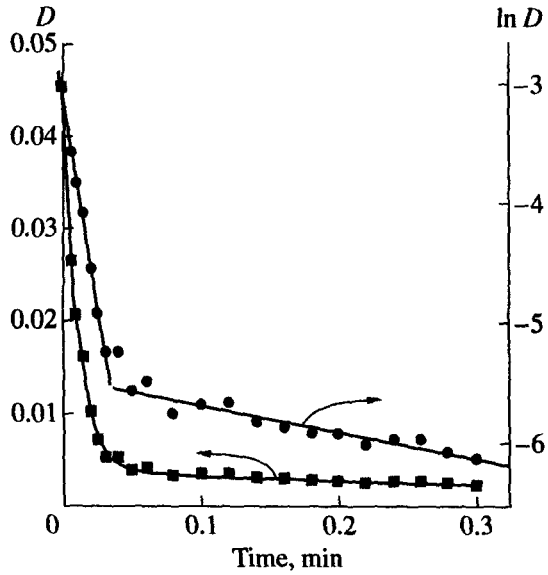

Fig. 5. Typical changes of absorbance D at $\lambda = 675$ nm and its linearization in semilogarithmic coordinates at $[Co]_\Sigma \geq 5 \times 10^{-5}$ mol/l ($[Ru^{3+}(bpy)_3]_0 = 5 \times 10^{-4}$ mol/l, 0.03 mol/l borate buffer at pH 9.2; the cell length is 0.2 cm).

proposed earlier [4, 5] was chosen for the quantitative kinetic description under the conditions of oxidant excess over the catalyst:

$$\text{Co(III)OH} + \text{Ru}^{3+}(\text{bpy})_3 \underset{}{\overset{K_1}{\rightleftharpoons}} \text{Co(III)O}\cdots\text{Ru}^{3+}(\text{bpy})_3 + \text{H}^+, \quad \text{(II)}$$

$$\text{Co(III)OH} + \text{Ru}^{2+}(\text{bpy})_3 \underset{}{\overset{K_2}{\rightleftharpoons}} \text{Co(III)O}\cdots\text{Ru}^{2+}(\text{bpy})_3 + \text{H}^+, \quad \text{(III)}$$

$$\text{Co(III)O}\cdots\text{Ru}^{3+}(\text{bpy})_3 \xrightarrow{k_3} \text{Co(IV)O} + \text{Ru}^{2+}(\text{bpy})_3, \quad \text{(IV)}$$

$$2\text{Co(IV)O} \xrightarrow{k_4} 2\text{Co(II)} + \text{O}_2, \quad \text{(V)}$$

$$\text{Co(II)} + \text{Ru}^{3+}(\text{bpy})_3 \xrightarrow[\text{H}_2\text{O}]{k_5} \text{Co(III)OH} + \text{Ru}^{2+}(\text{bpy})_3 + \text{H}^+, \quad \text{(VI)}$$

$$\text{Co(IV)O} + \text{Ru}^{2+}(\text{bpy})_3 \xrightarrow{k_6} \text{Co(III)OH} + \text{Ru}^{2+}(\text{bpy})_2(\text{bpy})_{ox}. \quad \text{(VII)}$$

Scheme 1.

Currently, it is commonly accepted that the step of first electron transfer (IV) from the catalyst active center to the oxidant is a rate-determining one. This was confirmed by quantum-chemical calculations [6, 7]. In this case, the concentrations of intermediate forms of the catalyst starting from step (V) can be considered stationary, and their fraction in the overall catalyst concentration is negligible. In this case, the reaction kinetics is largely determined by the fast equilibrium steps of ion-exchange adsorption (II) and (III) and the rate-limiting step of the first electron transfer (IV). The use of this scheme as a kinetic model enables the quantitative description of all of the experimental observations relevant to kinetics.

The oxidant is consumed in steps (IV) and (VI), but because step (IV) is the slowest, the rate of step (VI) is equal to the rate of step (IV). Of course, this is the case if the oxidant is largely consumed for water oxidation rather than for a side reaction. Then, the overall rate of water oxidation w can be described as follows:

$$w = 2k_3[\text{Co(III)O}\cdots\text{Ru}^{3+}(\text{bpy})_3]. \quad (1)$$

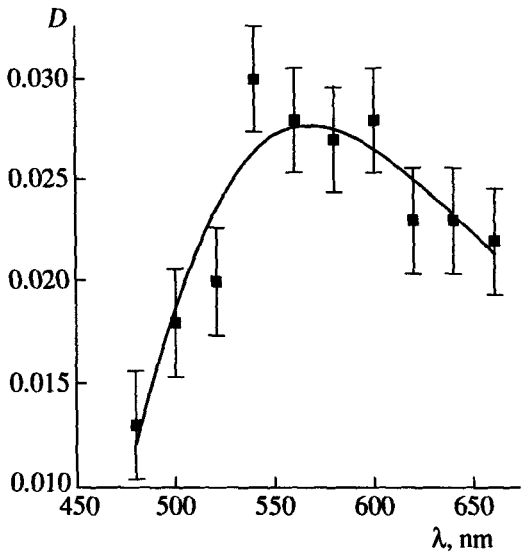

Fig. 6. Reconstructed spectra of the intermediate ($[Co]_\Sigma = 4 \times 10^{-4}$ mol/l, $[Ru^{3+}(bpy)_3]_0 = 5 \times 10^{-4}$ mol/l, 0.03 mol/l borate buffer at pH 9.2; the cell length is 0.2 cm).

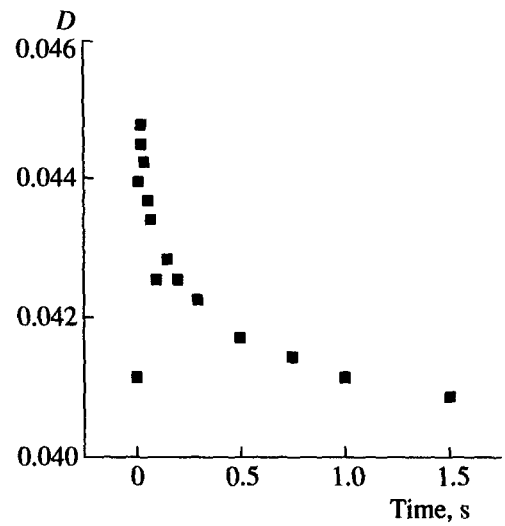

Fig. 7. Absorbance of the intermediate at $\lambda = 568$ nm vs. time (0.03 mol/l borate buffer, pH 9.2, $[Co]_\Sigma = 5 \times 10^{-5}$ mol/l, $[Ru^{3+}(bpy)_3]_0 = 1 \times 10^{-4}$ mol/l, and a cell length of 0.2 cm).

Because adsorption equilibria (II) and (III) are fast, the concentrations of the adsorbed forms of the oxidant and its reduced form are determined by the formulas

$$[\text{Co(III)O}\cdots\text{Ru}^{3+}(\text{bpy})_3] = K_1[\text{Co(III)OH}][\text{Ru}^{3+}(\text{bpy})_3]/[\text{H}^+] = K_1'[\text{Co(III)OH}][\text{Ru}^{3+}(\text{bpy})_3], \quad (2)$$

$$[\text{Co(III)O}\cdots\text{Ru}^{2+}(\text{bpy})_3] = K_2[\text{Co(III)OH}][\text{Ru}^{2+}(\text{bpy})_3]/[\text{H}^+] = K_2'[\text{Co(III)OH}][\text{Ru}^{2+}(\text{bpy})_3]. \quad (3)$$

As mentioned above, the contribution of Co(IV)O and Co(II) to the overall concentration is small. Therefore, taking into account formulas (2) and (3), we may write down the following expression:

$$[\text{Co}]_\Sigma \approx [\text{Co(III)OH}] + K_1'[\text{Co(III)OH}][\text{Ru}^{3+}(\text{bpy})_3] + K_2'[\text{Co(III)OH}][\text{Ru}^{2+}(\text{bpy})_3], \quad (4)$$

where $[\text{Co}]_\Sigma$ is the overall concentration of cobalt.

In this case, the concentration of free active centers of the catalyst is

$$[\text{Co(III)OH}] \approx [\text{Co}]_\Sigma/(1 + K_1'[\text{Ru}^{3+}(\text{bpy})_3] + K_2'[\text{Ru}^{2+}(\text{bpy})_3]), \quad (5)$$

and the overall reaction rate is

$$w \approx 2K_1'k_3[\text{Ru}^{3+}(\text{bpy})_3] \times [\text{Co}]_\Sigma/(1 + K_1'[\text{Ru}^{3+}(\text{bpy})_3] + K_2'[\text{Ru}^{2+}(\text{bpy})_3]). \quad (6)$$

A similar expression for the rate of reaction (I) was obtained in [5], but there was no direct experimental evidence for this expression.

It can be seen that in the case of the weak dependence of the denominator on the concentrations of both ruthenium complexes, equation (6) corresponds to the pseudo-first-order reaction with respect to concentration $\text{Ru}^{3+}(\text{bpy})_3$. The apparent pseudo-first-order rate constant of the water oxidation (or oxidant consumption) can be described as

$$k_{app} \approx 2K_1'k_3[\text{Co}]_\Sigma/(1 + K_1'[\text{Ru}^{3+}(\text{bpy})_3] + K_2'[\text{Ru}^{2+}(\text{bpy})_3] \quad (7)$$

or

$$\frac{1}{k_{app}} \approx \frac{1}{2k_3[\text{Co}]_\Sigma} \times \left(\frac{1}{K_1'} + [\text{Ru}^{3+}(\text{bpy})_3] + \frac{K_2'}{K_1'}[\text{Ru}^{2+}(\text{bpy})_3]\right). \quad (8)$$

Our experimental findings agree well with equations (7) and (8).

These equations describe the experimentally observed exponential character of kinetic curves on the time and deceleration of oxidant consumption closer to the end of reaction. Let us rewrite equation (8) as follows:

$$\frac{1}{k_{app}} \approx \frac{1}{2k_3[\text{Co}]_\Sigma} \times \left(\frac{1}{K_1'} + [\text{Ru}^{3+}(\text{bpy})_3]_0 + \left(\frac{K_2'}{K_1'} - 1\right)[\text{Ru}^{2+}(\text{bpy})_3]\right), \quad (9)$$

where $[\text{Ru}^{3+}(\text{bpy})_3]_0 = [\text{Ru}^{3+}(\text{bpy})_3] + [\text{Ru}^{2+}(\text{bpy})_3]$ is the initial concentration of the oxidant and $[\text{Ru}^{3+}(\text{bpy})_3]$ and $[\text{Ru}^{2+}(\text{bpy})_3]$ are the concentrations of its oxidized and reduced forms, respectively. Obviously, the form of these kinetic curves depends on the ratio between the adsorption equilibrium constants K_1' and K_2'. If the values of these constants are close, then we may expect for the colloidal catalyst that the third term in brackets is small relatively to the others, and the apparent rate constant should not indeed change during the reaction because it only depends on the initial concentration of the oxidant.

The observed small difference in the equilibrium constants of adsorption for the oxidized and reduced forms of ruthenium complexes can probably be explained by the specific features of the colloidal catalyst, which is starch-stabilized small particles of colloidal Co(III) hydroxide 2–10 nm in size [13], which are coated with starch molecules. In this case, the adsorption of ruthenium cationic complexes on the surface is largely controlled by steric factors. Both ruthenium complexes have rather bulky similar ligands. Therefore, the equilibrium constants of their adsorption should be lower than those for starch-free catalysts and similar to each other. As a consequence, the effect of retardation by the reduced oxidant form may not be as substantial in our case as in other systems studied.

Expression (8) describes the observed dependences of the apparent rate constant on the concentrations of the catalyst, oxidant, and its reduced form. Using this formula, we can estimate K_1', K_2', and k_3.

Let us consider the situation when the initial concentration of the $[\text{Ru}^{2+}(\text{bpy})_3]$ complex equals zero.

Assuming that $K_1 \approx K_2$ and rearranging equation (9), we have

$$\frac{1}{k_{app}} \approx \frac{1}{2K_1'k_3[Co]_\Sigma} + \frac{[Ru^{3+}(bpy)_3]_0}{2k_3[Co]_\Sigma}. \quad (10)$$

Using this equation and the dependence of k_{app} on the initial oxidant concentration, it is easy to estimate the constants K_1' and k_3. The value of k_3 can be calculated from the slope of the line on the plot of $1/k_{app}$ vs. $[Ru^{3+}(bpy)_3]_0$ (Fig. 3). Given the value of k_3, K_1' can be calculated as an intercept on the ordinate axis.

If the $[Ru^{2+}(bpy)_3]$ complex is added to the initial oxidant solution in an amount comparable to $[Ru^{3+}(bpy)_3]_0$, equation (8) can be rewritten as

$$\frac{1}{k_{app}} \approx \frac{1 + K_1'[Ru^{3+}(bpy)_3]}{2K_1'k_3[Co]_\Sigma} + \frac{K_2'[Ru^{2+}(bpy)_3]_0}{2K_1'k_3[Co]_\Sigma}. \quad (11)$$

Given the value of k_3, the intercept on the plot of $1/k_{app}$ vs. $[Ru^{2+}(bpy)_3]_0$ on the ordinate axis gives the value of K_1'. Then, the slope of the line and the values of K_1' and k_3 give the value of K_2'.

The results of calculation for two experimental series at pH 9.2 are shown in the table. These series were obtained for two catalyst samples prepared according to the same technique.

As can be seen from the table, the values of k_3 belong to a region of 10^2–10^3 s^{-1} and the values of K_1' belong to a region of 10^4–10^5 l/mol. The values of K_2' are ~1.5 times lower than K_1'. The differences in the parameters for the two experimental series are within the limits of experimental error. Moreover, these differences can be due to the fact that each experimental series was obtained with different catalyst samples, whose properties depend on the duration of their storage [8].

The possible nature of intermediates of the catalytic process. The use of cobalt hydroxide as an oxidation catalyst is only known for water oxidation by strong one-electron oxidants. However, cobalt and other transition metal complexes with various organic ligands are well known as catalysts for redox reactions with oxygen transfer [16]. In these reactions, oxygen activation is believed to occur via the formation of intermediate peroxo complexes. Based on the formal kinetic scheme (scheme 1 above) and taking into account that we found an intermediate which is most likely a cobalt peroxo complex, we propose the following detailed scheme of water oxidation over cobalt hydroxide (scheme 2).

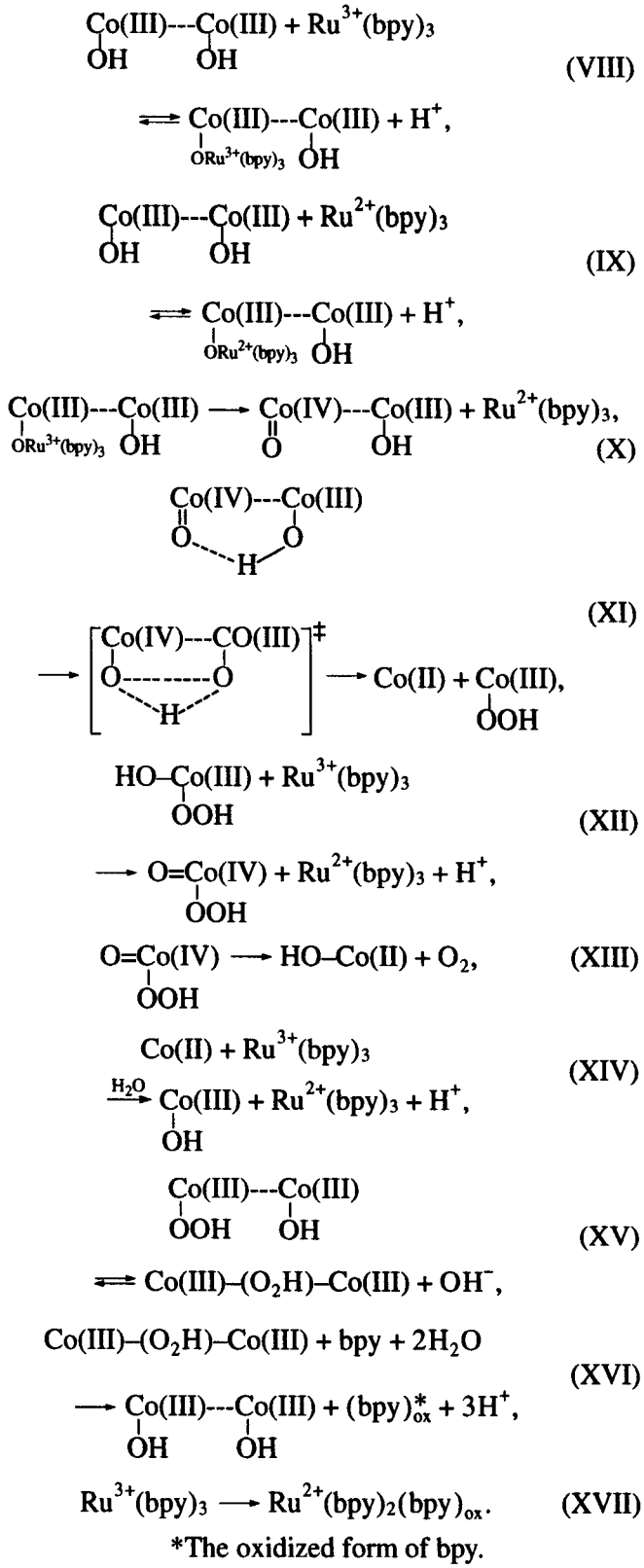

*The oxidized form of bpy.

Scheme 2.

Equations (VIII)–(X) in this scheme detail the corresponding equations of Scheme 1. Then, according to the results reported in [6, 7], oxo and hydroxyl groups, coordinated to two adjacent cobalt ions of the active center, react with each other. This interaction results in

Parameters K_1', K_2', and k_3 of water oxidation in 0.03 mol/l borate buffer at pH 9.2 and 298 K

No. of series	Reactant concentration, mol/l			k_3, s^{-1}	$K_1' \times 10^{-4}$, l/mol	K_2', l/mol
	$[Co]_\Sigma \times 10^6$	$[Ru^{3+}(bpy)_3]_0$	$[Ru^{2+}(bpy)_3]_0$			
1	5	5×10^{-5}–5×10^{-4}	0	1340	22	–
	25	10^{-5}–10^{-3}	0	1380	13	–
	5	2.5×10^{-4}	5×10^{-5}–5×10^{-4}	–	1.2	$0.92K_1'$
Average values				1360	12	$0.92K_1'$
2	5	10^{-5}–5×10^{-4}	0	142	3.2	–
	2.5	10^{-5}–5×10^{-4}	0	146	1.3	–
	2.5	2.5×10^{-6}	5×10^{-5}–5×10^{-4}	–	0.6	$0.62K_1'$
	5	5×10^{-6}	5×10^{-5}–5×10^{-4}	–	1.4	$0.67K_1'$
Average values				143	3.0	$0.65K_1'$

the formation of an O–O bond corresponding to the oxidation of water with the loss of two electrons, the simultaneous two-electron reduction of one of the cobalt ions, and the coordination of a peroxide group to another cobalt ion. Obviously, the polynuclear structure of the hydroxide catalyst should be favorable for this process.

The cobalt ion with the coordinated peroxide group may react with another $Ru^{3+}(bpy)_3$ complex being oxidized to Co(IV) by reaction (XII). Then, the peroxo group coordinated to the cobalt ion is oxidized in the process of two-electron transfer in reaction (XIII). As a result, water is oxidized to form molecular oxygen and two Co(II) centers (steps (XI) and (XIII)). Co(II) remains in the structure of Co(III) hydroxide. The catalytic cycle is completed by Co(II) reoxidation by $Ru^{3+}(bpy)_3$ to form Co(III) accompanied by the fast addition of the hydroxyl group (reaction (XIV)), and the catalyst returns to its initial state.

The intermediate found in this work is consumed with a rate constant that is 2–3 orders of magnitude lower than the apparent rate constant of the rate-determining step (X). Therefore, it cannot participate in the steps of O_2 formation. We assume that, unlike a terminal peroxo complex, the formation of which should be expected in step (XI), the intermediate observed is a long-lived bridging peroxo complex.

It has been found [17] that the oxidative elimination of O_2 from bridging cobalt peroxides is impossible because these peroxides are oxidized by all known oxidants with the loss of one electron and the formation of a bridging superoxide. Moreover, like our intermediate, bridging cobalt peroxides of different structures have low-intensity absorption bands at 500–600 nm because their main adsorption bands are in the near UV region [16, 18]. Finally, Mahroof-Tahir *et al.* [19] described the difference in the redox properties of peroxo copper complexes: the terminal peroxo group is oxidized to form O_2, but the bridging group (as in the case of cobalt) is a rather strong oxidant. In our scheme, the bridging peroxide is formed by reaction (XV). The formation of bridging peroxide should inhibit water oxidation and favor side processes of bipyridyl oxidation (XVI). In an alkaline media, equilibrium (XV) should shift to the left because of competition with hydroxyl groups. This should result in an increase in the O_2 yield, and this is observed in the experiment.

Scheme 2 also has a reaction of spontaneous oxidant destruction (XVII). The contribution of this step to a decrease in the O_2 yield becomes noticeable at low catalyst concentrations. This reaction was studied in detail in [1, 5, 20].

The scheme suggested in this work involves two coupled catalytic processes of water oxidation and bipyridyl catalytic destruction. The ratio between the rates of these two processes and the ratio between the product yields depend on the ratio between the concentrations of peroxide intermediates, which in turn depends on the reaction conditions. An increase in pH should favor reaction (XII), shift equilibrium (VIII) to the right, and increase the yield of oxygen, which is observed in the experiment (Fig. 1). An increase in the catalyst concentration to values comparable to the oxidant concentrations results in a decrease in the yield of

oxygen (Fig. 1). This can easily be explained by the fact that the probability of oxidant interaction with the same active center (XII) for the second time decreases with an increase in the catalyst concentration. Therefore, more terminal peroxo complexes, which are active in water oxidation, will transform into bridging peroxo complexes, which are active in the side reaction.

CONCLUSION

New data on the mechanism of water oxidation were obtained due to the use of the colloidal form of cobalt hydroxide. The use of this catalyst form allowed us to show experimentally that the oxidant and its reduced form compete for adsorption sites on the catalyst surface. We found conditions under which the adsorption of the reduced oxidant form only slightly affects the kinetics of water oxidation. We found the values of adsorption equilibrium constants for the oxidant and its reduced form and the rate constants of rate-determining steps for both coupled reaction pathways (water oxidation to molecular oxygen and catalytic bipyridyl destruction). We found the intermediate, activated form of oxygen on the catalyst surface. This is a peroxo group coordinated to cobalt ions in the composition of cobalt hydroxide. Based on the experimental data, we proposed the mechanism which most exactly describes molecular processes during oxygen formation from water in artificial systems and may help to understand oxygen formation in the oxygen-forming complex of photosystem II of green plants.

REFERENCES

1. Gosh, P.K., Brunschiwig, B.S., Chou, M., *et al.*, *J. Am. Chem. Soc.*, 1984, vol. 106, no. 17, p. 4772.
2. Brunschiwig, B.S., Chou, M., Creutz, C., and Sutin, N., *J. Am. Chem. Soc.*, 1983, vol. 105, no. 14, p. 4832.
3. Moravskii, A.P., Khannanov, N.K., Khramov, A.V., *et al.*, *Khim. Fiz.*, 1984, vol. 3, no. 11, p. 1584.
4. Elizarova, G.L., Gerasimov, O.V., Matvienko, G.L., *et al.*, *Izv. Sib. Otd. Akad. Nauk SSSR, Ser. Khim. Nauk*, 1990, no. 3, p. 94.
5. Gerasimov, O.V., *Cand. Sci. (Chem.) Dissertation*, Novosibirsk: Inst. of Catalysis, 1988.
6. Filatov, M.J., Elizarova, G.L., Zhidomirov, G.M., and Parmon, V.N., *J. Molec. Catal.*, 1994, vol. 91, no. 1, p. 71.
7. Parmon, V.N., Elizarova, G.L., and Zhidomirov, G.M., *11th Int. Conf. on Photochemical Conversion and Storage of Solar Energy (IPS-11)*, Bangolore, 1996, p. 33.
8. Elizarova, G.L., Matvienko, L.G., Pestunova, O.P., and Parmon, V.N., *Kinet. Katal.*, 1994, vol. 35, no. 3, p. 362.
9. Lur'e, Yu.Yu., *Spravochnik po analiticheskoi khimii* (Handbook on Analytical Chemistry), Moscow: Mir, 1969.
10. Liu, C.F., Liu, N.C., and Bailar, J.C., *Inorg. Chem.*, 1964, vol. 3, no. 8, p. 1085.
11. Creutz, C. and Sutin, N., *Proc. Natl. Acad. Sci. U.S.A.*, 1975, vol. 72, no. 8, p. 2855.
12. Mori, M., Shibata, M., and Kyuno, E., *Bull. Chem. Soc. Jpn.*, 1956, vol. 29, p. 883.
13. Elizarova, G.L., Matvienko, L.G., Taran, O.P., *et al.*, *Kinet. Katal.*, 1992, vol. 33, no. 4, p. 898.
14. Khannanov, N.K. and Shafirovich, V.Ya., *Kinet. Katal.*, 1981, vol. 22, no. 1, p. 248.
15. Khannanov, N.K., Khramov, A.V., Moravskii, A.P., and Shafirovich, V.Ya., *Kinet. Katal.*, 1983, vol. 24, no. 4, p. 858.
16. Bratushko, Yu.I., *Koordinatsionnye soedineniya 3d-perekhodnykh metallov s molekulyarnym kislorodom* (Coordination Compounds of 3*d* Transition Metals with Molecular Oxygen), Kiev: Naukova Dumka, 1987.
17. Sykes, A.G. and Weil, J.A., *Prog. Inorg. Chem.*, 1970, vol. 13, p. 1.
18. Hoffman, A.B. and Taube, H., *Inorg. Chem.*, 1968, vol. 7, no. 10, p. 1971.
19. Mahroof-Tahir, M., Murthy, N.N., Karlin, K.D., *et al.*, *Inorg. Chem.*, 1992, vol. 31, no. 14, p. 3000.
20. Gerasimov, O.V., Elizarova, G.L., and Parmon, V.N., *Izv. Akad. Nauk SSSR, Ser. Khim.*, 1988, no. 6, p. 1243.